Original Article

Variations of arterial compliance and vascular resistance due to plaque or infarct in a single vascular territory of the middle cerebral artery

Wenwen Chen[1#], Xiaowei Song[2#], Hanyu Wei[1], Mingzhu Fu[1], Shuo Chen[1], Chenming Wei[2], Zhuozhao Zheng[3], Jian Wu[2,4], Rui Li[1]

[1]Center for Biomedical Imaging Research, Department of Biomedical Engineering, School of Medicine, Tsinghua University, Beijing, China; [2]Department of Neurology, Beijing Tsinghua Changgung Hospital, School of Clinical Medicine, Tsinghua University, Beijing, China; [3]Department of Radiology, Beijing Tsinghua Changgung Hospital, Beijing, China; [4]IDG/McGovern Institute for Brain Research at Tsinghua University, Beijing, China

Contributions: (I) Conception and design: W Chen, R Li; (II) Administrative support: J Wu, R Li; (III) Provision of study materials or patients: Z Zheng, X Song; (IV) Collection and assembly of data: J Wu, X Song, C Wei; (V) Data analysis and interpretation: W Chen, X Song, H Wei, M Fu, S Chen; (VI) Manuscript writing: All authors; (VII) Final approval of manuscript: All authors.

[#]These authors contributed equally to this work.

Correspondence to: Rui Li, PhD. Center for Biomedical Imaging Research, Department of Biomedical Engineering, School of Medicine, Tsinghua University, No. 30 Shuangqing Road, Haidian District, Beijing 100084, China. Email: leerui@tsinghua.edu.cn; Jian Wu, PhD. Department of Neurology, Beijing Tsinghua Changgung Hospital, No.168 Litang Road, Changping District, Beijing 102218, China; IDG/McGovern Institute for Brain Research at Tsinghua University, No. 30 Shuangqing Road, Haidian District, Beijing 100084, China. Email: wujianxuanwu@126.com.

Background: Arterial compliance (AC) and vascular resistance (VR) are crucial for the regulation capacity of the vascular system. However, alterations of these features and hemodynamics due to atherosclerosis in a single intracranial artery territory have not been extensively investigated. Thus this study aimed to examine the AC, VR, and hemodynamic variations due to plaque and infarction in the middle cerebral artery (MCA).

Methods: Patients with symptomatic MCA atherosclerosis were recruited. Both sides of the MCA were assessed and then classified according to the following scheme: group 0, without plaque; group 1, with plaque but without infarct; group 2, with plaque and infarct in the supplying territories. Data on AC, VR, blood flow, and pulsatility index (PI) were obtained based on 4D flow magnetic resonance imaging (MRI) and the Windkessel model.

Results: A total of 63 patients were recruited. After 17 MCAs were excluded (occlusion, n=6; poor image quality, n=11), datasets on 109 MCAs were finally collected and classified into group 0 (n=39), group 1 (n=40), and group 2 (n=30). From groups 0 to 2, there was a decrease in AC (0.0060±0.0031 *vs.* 0.0052±0.0029 *vs.* 0.0026±0.0020 mL/mmHg) and an increase in VR [28.65±16.11 *vs.* 42.59±27.53 *vs.* 63.21±40.37 mmHg/(mL/s)]. Compared to group 1, group 2 had significantly decreased AC (0.0052±0.0029 *vs.* 0.0026±0.0020 mL/mmHg; P=0.003) and increased VR [42.59±27.53 *vs.* 63.21±40.37 mmHg/(mL/s); P=0.021]. From group 0 to group 2, there was a decrease in blood flow (179.29±73.57 *vs.* 125.11±59.04 *vs.* 92.05±48.79 mL/min; P<0.001). The PI varied significantly among the 3 groups (0.86±0.20 *vs.* 1.12±0.50 *vs.* 0.79±0.16; P<0.001), with group 1 having the highest PI.

Conclusions: With the occurrence of plaque and infarct, AC and blood flow progressively decrease while VR increases. The PI was the highest in the group with plaque and without infarct. Assessments of vascular function and hemodynamics in a single artery territory can clarify comprehensive alterations in the cerebral vascular system (CVS).

Keywords: Arterial compliance (AC); blood flow pulsatility; 4D flow magnetic resonance imaging (4D flow MRI); intracranial atherosclerosis disease (ICAD); vascular resistance (VR)

Submitted Mar 14, 2023. Accepted for publication Sep 06, 2023. Published online Oct 25, 2023.
doi: 10.21037/qims-23-222
View this article at: https://dx.doi.org/10.21037/qims-23-222

Introduction

Intracranial atherosclerosis disease (ICAD) is increasingly being acknowledged as the most predominant risk factor for ischemic stroke (1). ICAD causes physiological changes in the vessel wall that are likely to impair the functions of the cerebral vascular system (CVS) (2,3). With the impaired function of the CVS, cerebral hemodynamics are likely to be altered in turn (4), and conversely, these altered hemodynamics may also affect the structure or function of the CVS (5). Therefore, there may be a two-way interaction between cerebral hemodynamics and CVS function, and it is thus critical to investigate the overall alteration of the CVS, which may include both cerebral hemodynamics and the functions of the CVS. However, the relationship between ICAD and the overall alteration of the CVS has not been intensely studied. ICAD may co-exist with infarction or not. There may be considerable benefit in examining the differences in overall alteration across 3 conditions: healthy vessels, atherosclerotic vessels without ipsilateral infarction, and atherosclerotic vessels with ipsilateral infarction.

CVS function is mainly characterized by cushioning and the conduit functions (6). The cushioning function is assessed via arterial compliance (AC) (6), while the conduit function is assessed via vascular resistance (VR) (6,7). The Windkessel model is widely used as a noninvasive method to assess both AC and VR (8).

Previous research has attempted to assess CVS function, however, with limitations: (I) first, the investigation of the relationship between AC and atherosclerosis has mainly been conducted in extracranial arteries (2,9), with intracranial arteries being mostly ignored. (II) Second, previous studies did not measure AC and plaque at the same location, which reduced the association of AC with atherosclerosis (10). Therefore, an investigation of AC and atherosclerosis in the same intracranial artery territory is needed. The middle cerebral artery (MCA), as one, main intracranial artery, is a suitable subject for such a study, as MCA is the most common pathologically affected blood vessel in the brain and has considerable clinical significance (11). Moreover, the MCA is one of the arteries most frequently involved in stroke (12). One previous study also indicated that atherosclerosis in large intracranial arteries, especially the MCA, is common cause of ischemic stroke in Asians (13). Considering the clinical significance and high prevalence of MCA in atherosclerosis, we chose it as a region of interest in this analysis. (III) Third, it is rare for previous studies to obtain AC and VR together in assessing CVS function or to do so only either in silico or *in vivo* (14-16).

AC and VR can regulate the hemodynamics of CVS, including blood flow and pulsatility (16). Acquiring AC, VR, and concomitant hemodynamics data is pivotal to studying the overall CVS alterations and their interactive impact. Comprehensive CVS alterations including AC, VR, and hemodynamics have not been reported in relation to atherosclerosis disease, especially in ICAD. Furthermore, ICAD may possibly cause infarction, and CVS alteration may differ between circumstances of plaque and infarct; however, this has not been clarified by research.

Transcranial Doppler (TCD) and 2-dimensional phase contrast magnetic resonance imaging MRI (2D PC-MRI) are widely used methods for characterizing cerebral hemodynamics. However, the TCD technique is limited by the acoustic windows of the head, and 2D PC-MRI, which assesses each artery separately, is time-consuming (16). The emergence of 4D flow MRI can overcome some of these, and it is possible to simultaneously obtain time-resolved 3D quantitative blood flow information of the main intracranial arteries (17,18). Therefore, 4D flow MRI was the method of choice for this study.

The hypothesis of this study is that the overall CVS alterations, including vascular functions and hemodynamics, are related to the occurrence of atherosclerosis or infarction. In this study, we focused on a single intracranial

artery territory, the MCA, to clarify the relationship between ICAD and overall CVS alterations. This study aimed to investigate AC, VR, and concomitant variations in hemodynamics due to atherosclerosis or infarction in MCA based on 4D flow MRI and the Windkessel model. We present this article in accordance with the STROBE reporting checklist (available at https://qims.amegroups.com/article/view/10.21037/qims-23-222/rc).

Methods

Participants

Patients with symptomatic MCA atherosclerosis were prospectively and consecutively screened in a comprehensive stroke center (Tsinghua Changgung Advanced Stroke Center, Beijing Tsinghua Changgung Hospital). Inclusion criteria for patients with ischemic stroke were the following: (I) patients were within 4 weeks of symptom onset; (II) patients had MCA atherosclerosis; (III) if infarction occurred, the MCA atherosclerosis was on the ipsilateral side of the infarct; (IV) patients were out of the time window of intravenous thrombolytic therapy, nor receive thrombectomy therapy; and (V) patients had no contraindications to MRI. The exclusion criteria were the following: (I) ischemic stroke symptoms caused by cardioembolism, (II) carotid artery stenosis (>50%) indicated by vascular imaging examination, (III) with nonatherosclerotic diseases (such as vasculitis, moyamoya disease, or dissection) suggested by vessel wall imaging, (IV) a history of stent placement or endovascular treatment, and (V) with chronic infarcts.

Taking MCAs as the basic elements, we reviewed the bilateral MCAs in each participant and excluded MCAs if (I) the M1 segment was occluded and resulted in an undetectable flow from 4D flow MRI or if (II) there was poor image quality of 4D flow MRI [including motion artifacts, phase wrapping, or low signal-to-noise ratio (SNR)]. The M1 segment is defined as the MCA segment that extends from the end of the internal carotid artery, perforating the brain up to its division (11). Clinical and demographic information, including sex, age, vascular risk factors (hypertension, diabetes mellitus, hyperlipidemia, and current smoking), and blood pressure were recorded for each patient. Hyperlipidemia was diagnosed based on the adult treatment panel III guidelines (19,20) [total cholesterol ≥240 mg/dL, low-density lipoprotein cholesterol (LDL-C) ≥160 mg/dL or high-density lipoprotein cholesterol (HDL-C) <40 mg/dL] or on the use of lipid-lowering medication.

Standard protocol approval, registration, and patient consent

The Ethics Review Board of the Beijing Tsinghua Changgung Hospital approved the study protocols, and the study was performed in accordance with the guidelines of the Declaration of Helsinki (as revised in 2013). Written informed consent was obtained from each patient or their legal guardians.

MRI protocol

All patients were scanned by a 3.0T MR scanner (Discovery 750, GE HealthCare, Chicago, IL, USA). The MRI protocol included routine brain MRI [including T1-weighted (T1W), T2W, fluid-attenuated inversion recovery (FLAIR), diffusion-weighted imaging (DWI)], 4D flow MRI, pre- and post-contrast 3D cube-T1W MRI (vessel wall imaging), and 3D time-of-flight magnetic resonance angiography (TOF MRA). The parameters of 4D flow MRI were the following: Cartesian image acquisition with repetition time/time to echo (TR/TE) =5.01/2.36 ms, flip angle =14°, and velocity encoding (VENC) =150 cm/s in all directions (as velocities that exceed 120 cm/s may increase due to the stenosis (21), VENC was set higher to 150 cm/s), spatial resolution =1×1×1 mm^3, and temporal resolution =30–57 ms. Parameters for 3D cube-T1W MRI were the following: coronal plane scan, TR/TE =800/16 ms, flip angle =90°, field of view (FOV) =23×18.4 cm^2, and spatial resolution =0.7×0.6×0.6 mm^3.

Imaging analysis and group classification

The presence of MCA-M1 plaque, defined as eccentric thickening of the arterial wall (2), was identified by 2 radiologists based on TOF and cube images, using RadiAnt (Medixant, Poznan, Poland). In the case of disagreement, the assessment was conducted by a third senior radiologist. Infarction was recognized as hyperintensity on DWI. In this analysis, whether a new infarct was present in the MCA supplying territories ipsilateral to the atherosclerotic MCA was identified by 2 experienced radiologists based on published criteria (22). The MCAs were then classified into 3 groups: (I) MCA without plaque (group 0), (II) MCA with plaque but without infarct in its supplying territories

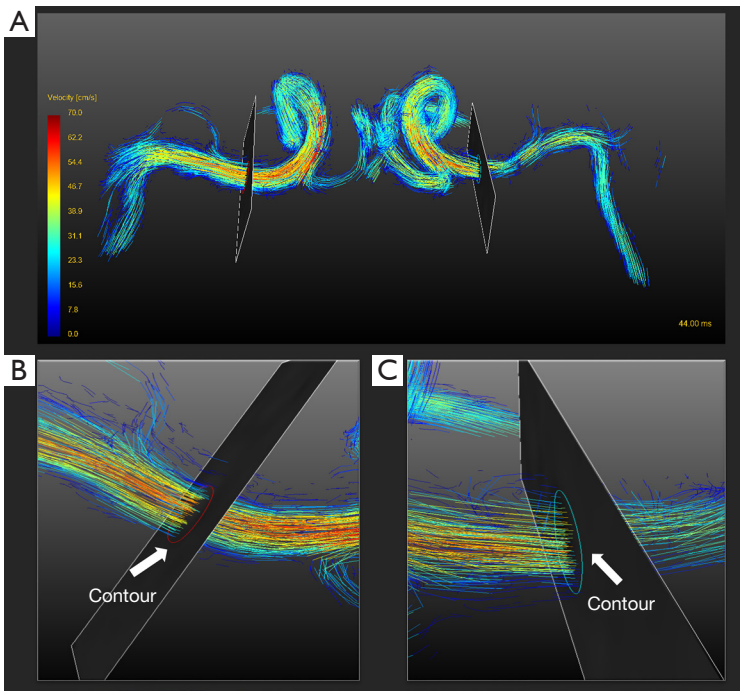

Figure 1 Blood flow measurements using GTFlow software. (A) Flow pattern visualization was performed with streamlines. For flow quantification, cut planes of the MCA-M1 segment were created perpendicular to the proximal M1 segment. (B,C) Contours were drawn in cut planes to complete hemodynamic measurements (11). MCA, middle cerebral artery; MCA-M1, the MCA segment extending from the end of the internal carotid artery and perforating the brain up to its division.

(group 1), and (III) MCA with plaque and ipsilateral infarct in its supplying territories (group 2). Different groups could have MCAs from the same patient, and the overlap could reduce the influence of individual hemodynamic variations to some extent. In the case of overlap, it is more persuasive if the results are still significantly different.

All postprocessing steps for 4D flow MRI, including eddy-current correction, phase unwrapping, vessel mask generation, flow visualization, and quantification, were performed in GTFlow version 3.2.8 (GyroTools, Zurich, Switzerland) (23). The MCA vessel structure was segmented from 4D flow MRI using velocity-weighted masks. Streamlines were used for blood flow visualization. For flow quantification, cut planes of the MCA-M1 segment were created perpendicularly to the proximal M1 segment as shown in *Figure 1*. Measuring the through-plane flow in curved vessels requires the ability to reslice the data volume perpendicularly to the vessel axis. GTFlow can reslice the flow dataset and help interactively plan the orientation and position of the resliced stack (cut plane). First, the cut plane was created in the position of the proximal and relatively straight section of the MCA-M1. If there was atherosclerosis in the MCA-M1, the cut planes were set proximal to the stenosis. The orientation of the cut plane was then adjusted to make it perpendicular to the vessel from 3 dimensions. Contours were drawn in cut planes to measure cerebral blood flow in a cardiac cycle. The average velocity and max velocity were also recorded at the proximal part of the MCA-M1.

Measurements of the average diameter of MCA-M1 in each group were obtained. The diameters were measured at 3 sites from the proximal section to the distal part of MCA-M1 using RadiAnt. If there was stenosis, the measurement sites were the narrowest stenosis and 2 other normal sites that were distal and proximal to the narrowest site. The average diameter of the MCA in each patient was then calculated as the average of the 3 diameters.

AC, VR, and hemodynamics measurements

In the 2-element Windkessel (2WK) model, AC and VR are represented as capacitance term C_{wk} and resistance term R, respectively, in the circuit (7). We assumed that maximum

blood pressure [BP_{max} (mmHg)] and the minimum blood pressure [BP_{min} (mmHg)] of the MCA were 0.7 times the values of systolic blood pressure [SBP (mmHg)] and diastolic blood pressure [DBP (mmHg)] according to previous studies (16,24,25). The pulse pressure amplitude of the blood pressure in the MCA (PP_{MCA}, mmHg) was defined as the difference between BP_{max} and BP_{min}. Based on the 2WK model, R [mmHg/(mL/s)] can be calculated as Eq. [1]. The mean arterial pressure in the MCA (MAP_{MCA}) was approximated as follows: $MAP_{MCA} = BP_{min} + 1/3\ PP_{MCA}$ (9,16). Based on the principle of circuits, C_{wk} (mL/mmHg) was expressed as Eq. [2] (16).

Mean blood flow (Q_{mean}, mL/min), maximum blood flow (Q_{max}, mL/min), and minimum blood flow (Q_{min}, mL/min) of the contours in the cut planes were measured using GTFlow. The inter- and intrarater reproducibility of flow measurements were conducted, with Q_{mean} being used for the validation. The pulsatility index (PI) is a commonly used as a noninvasive imaging biomarker of blood flow pulsatility and can be derived from blood flow information in a single cardiac cycle (4). In this study, PI was calculated according to the formula in Eq. [3] (16).

$$R = \frac{60 * MAP_{MCA}}{Q_{mean}} \quad [1]$$

$$C_{WK} = \frac{\sqrt{\left(\frac{MAP_{MCA} * \Delta Q}{PP_{MCA} * Q_{mean}}\right)^2 - 1}}{\frac{MAP_{MCA} * \omega * 60}{Q_{mean}}} \quad [2]$$

$$PI = \frac{Q_{\max} - Q_{\min}}{Q_{mean}} = \frac{\Delta Q}{Q_{mean}} \quad [3]$$

BP_{max}, maximum blood pressure of the middle cerebral artery; BP_{min}, minimum blood pressure of the middle cerebral artery; SBP, systolic blood pressure; DBP, diastolic blood pressure; PP_{MCA}, pulse pressure amplitude of the blood pressure in middle cerebral artery; MAP_{MCA}, the mean arterial pressure in the middle cerebral artery.

To strengthen the study, a measurement of arterial stiffness based on local pulse wave velocity (PWV) was determined using the Bramwell-Hill equation according to the calculation of AC in the literature (26), with Eqs. [4] and [5] being the corresponding equations. Units of arterial diameter and pressure were recorded as millimeters and millimeters of mercury (mmHg), respectively. Blood density (ρ) was assumed to be constant (1,059 kg/m^3). In this study, ΔP was equal to PP_{MCA}, and ΔD was measured based on 4D flow MRI using RadiAnt. The diameters of diastole and systole in proximal M1 segment were measured 3 times and averaged.

$$AC = \frac{\Delta D}{\Delta P} \quad [4]$$

$$PWV_{AC} = \sqrt{\frac{D_d^2 * 133.322}{\rho * AC * (2 * D_d + \Delta D)}} \quad [5]$$

ΔD, the change in arterial diameter between diastole and systole; ΔP, the change in local blood pressure; D_d, the arterial diameter at end-diastole; PP_{MCA}, pulse pressure amplitude of the blood pressure in the middle cerebral artery.

Statistical analysis

All quantitative variables are presented as the mean ± standard deviation (SD). Continuous parameters were compared among groups using analysis of variance (ANOVA) or the independent samples *t*-test. Categorical variables were compared using χ^2-test. Hemodynamic differences between the sexes were tested using the independent samples *t*-test. For pair-wise comparisons between groups, binary logistic regression analysis was used to adjust for the demographic and clinical confounding factors (P<0.1). The correlation between C_{wk} and PWV_{AC} was tested using Pearson correlation coefficient. Inter- and intrarater reproducibility of flow measurement was determined using Bland-Altman plots. Statistical analysis was conducted by MedCalc version 15.2.2 (MedCalc Software, Mariakerke, Belgium) and SPSS 26.0 (IBM Corp., Armonk, NY, USA). The level of statistical significance was set at P<0.05.

Results

Basic data

The flow diagram for participant recruitment is shown in *Figure 2*. A total of 87 patients were initially recruited, of whom 24 were later excluded (carotid artery stenosis, n=15; cardio embolism, n=4; chronic infarcts, n=5). Ultimately, 63 patients were enrolled into the study. In the MCA selection process, among all 126 MCAs, 17 MCAs were

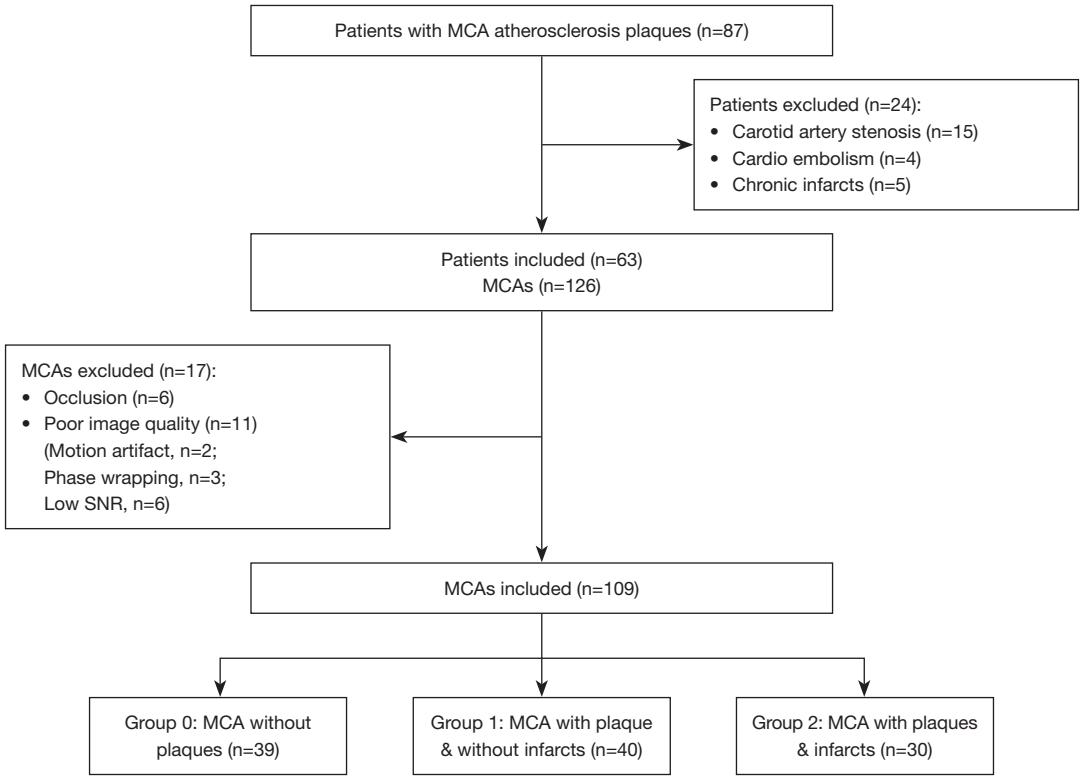

Figure 2 The flow diagram for the recruitment of patients and group classification. MCA, middle cerebral artery; SNR, signal-to-noise ratio.

excluded (MCA occlusion, n=6; poor image quality, n=11), and the remaining 109 MCAs were divided into groups of (I) MCA without plaque (group 0, n=39), (II) MCA with plaque but without infarct (group 1, n=40), and (III) MCA with plaque and ipsilateral infarct in the supplying territories (group 2, n=30). The other demographic and clinical characteristics of the 3 MCA groups are listed in *Table 1*. Except for sex and hyperlipemia, no significant differences was found among the 3 MCA groups. The demographic and clinical variables that needed to be adjusted as confounding factors (P<0.1) were diabetes, sex, and hyperlipemia. Compared with other groups, group 1 had a greater proportion of MCAs from male participants (P=0.03). In this study, there was no significant difference between males and females. As previous research indicates that women tend to have a higher PI than men (9), overrepresentation of males in group 1 was likely not the reason for the significant difference. Hemodynamic differences were not significant between males and females (males=73, females=36; Q_{mean}: 137.4±66.6 *vs.* 131.4±79.2 mL/min, P=0.70; PI: 0.97±0.42 *vs.* 0.87±0.21, P=0.1). The average diameter in the 3 MCA groups was significantly different (3.4754±0.5462 *vs.* 2.6725±0.5558 *vs.* 2.3777±0.5824; P<0.01).

Cwk, R, and hemodynamic parameters

The difference in C_{wk} among the 3 MCA groups was significant (0.0060±0.0031 *vs.* 0.0052±0.0029 *vs.* 0.0026±0.0020 mL/mmHg; P<0.001), as summarized in *Table 1*, with group 2 having the lowest C_{wk}. There was a decrease in C_{wk} from group 0 to group 2. Detailed pairwise comparison results of C_{wk} after adjustment for confounding factors are shown in *Figure 3*. Compared with MCA without plaque (group 0), MCA with plaque and without infarct (group 1) had a slightly decreased C_{wk} [0.0060±0.0031 *vs.* 0.0052±0.0029 mL/mmHg; odds ratio (OR) =0.00; P=0.348], but the difference was not significant. Compared with MCA with plaque and without infarct (group 1), MCA with plaque and infarct (group 2) had a significantly lower C_{wk} (0.0052±0.0029 *vs.* 0.0026±0.0020 mL/mmHg; OR =0.00; P=0.003).

The difference in R among the 3 MCA groups

Table 1 Comparisons of parameters among the 3 MCA groups

Parameters	Group 0 (n=39)	Group 1 (n=40)	Group 2 (n=30)	P
Age (years)	56±12	58±11	55±14	0.47
Male	23 (59.0)	33 (82.5)	17 (56.7)	0.031*
Hypertension	22 (56.4)	30 (75.0)	20 (66.7)	0.22
Diabetes	13 (33.3)	22 (55.0)	10 (33.3)	0.086
Hyperlipemia	10 (25.6)	24 (60.0)	8 (26.7)	0.0021*
CHD	2 (5.1)	4 (10.0)	1 (3.3)	0.49
Ever smoker	17 (43.6)	23 (57.5)	14 (46.7)	0.32
Ever drinker	15 (38.5)	19 (47.5)	12 (40)	0.83
SBP (mmHg)	138±21	136±21	141±20	0.57
DBP (mmHg)	80±14	76±9	82±14	0.15
R [mmHg/(mL/s)]	28.65±16.11	42.59±27.53	63.21±40.37	<0.001*
C_{wk} (mL/mmHg)	0.0060±0.0031	0.0052±0.0029	0.0026±0.0020	<0.001*
Q_{mean} (mL/min)	179.29±73.57	125.11±59.04	92.05±48.79	<0.001*
PI	0.86±0.20	1.12±0.50	0.79±0.16	<0.001*
PWV_{AC} (m/s)	8.86±2.42	15.29±4.26	22.47±8.82	<0.001*
Average diameter (mm)	3.48±0.55	2.67±0.56	2.38±0.58	<0.01*
Average velocity (cm/s)	29.70±8.33	28.69±11.81	25.50±12.26	0.26
Max velocity (cm/s)	65.79±21.54	72.37±30.12	51.06±28.88	<0.01*

Data are presented as mean ± SD or n (%). *, P<0.05. Group 0, MCA without plaque (n=39); Group 1, MCA with plaque and without infarct (n=40); Group 2, MCA with plaque and infarct (n=30); MCA, middle cerebral artery; CHD, coronary heart disease; SBP, systolic blood pressure; DBP, diastolic blood pressure; PWV_{AC}, pulse wave velocity; AC, arterial compliance.

was also significant [28.65±16.11 *vs.* 42.59±27.53 *vs.* 63.21±40.37 mmHg/(mL/s); P<0.001], as shown in *Table 1*. R increased from group 0 to group 2. Pairwise comparison results of R after adjustment for confounding factors are shown in *Figure 3*. Compared with group 0, group 1 had a higher R [28.65±16.11 *vs.* 42.59±27.53 mmHg/(mL/s); OR =1.03; P=0.053]. Compared with group 1, group 2 had a significantly higher R [42.59±27.53 *vs.* 63.21±40.37 mmHg/(mL/s); OR =1.024; P=0.021].

Differences of Q_{mean} among the 3 MCA groups were also significant (179.29±73.57 *vs.* 125.11±59.04 *vs.* 92.05±48.79 mL/min; P<0.001), as indicated in *Table 1*. Q_{mean} showed an obvious decrease from group 0 to group 2. After adjustment for confounding factors, the pairwise comparison of Q_{mean} (*Figure 3*) showed significant differences in Q_{mean} between group 0 and group 1 (179.29±73.57 *vs.* 125.11±59.04 mL/min; OR =0.99; P=0.006) and between group 1 and group 2 (125.11±59.04 *vs.* 92.05±48.79 mL/min; OR =0.98; P=0.007). Bland-Altman plots of inter- and intrarater reproducibility of Q_{mean} are shown in *Figure 4*. The maximum velocities of groups 0–2 were 65.79±21.54, 72.37±30.12, and 51.06±28.88 cm/s, respectively (P<0.01), while their average velocities were 29.70±8.33, 28.69±11.81, and 25.50±12.26 cm/s, respectively (P=0.26), as shown in *Table 1*.

Differences of PI among the 3 MCA groups were also significant (0.86±0.20 *vs.* 1.12±0.50 *vs.* 0.79±0.16; P<0.001), but PI showed no unidirectional tendency. Group 1 (MCA with plaques and no infarct in DWI) had the highest PI among the groups (*Table 1*). After adjustment for confounding factors, pairwise comparison of PI (*Figure 3*) also showed significant differences in PI between group 0 and group 1 (0.86±0.20 *vs.* 1.12±0.50; OR =11.05; P=0.046) and between group 1 and group 2 (1.12±0.50 *vs.* 0.79±0.16; OR =0.018; P=0.012).

Local PWV_{AC} was significantly different among the

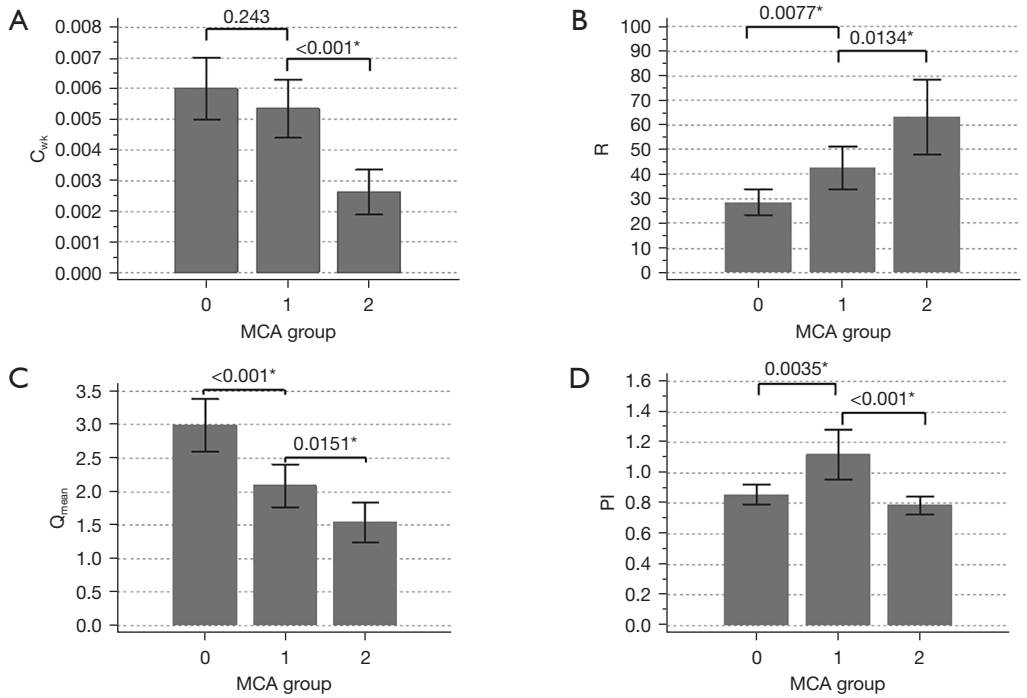

Figure 3 Pairwise comparisons of C_{wk}, R, and hemodynamic parameters including Q_{mean} and PI. Pairwise comparisons were made between group 0 (MCA without plaque) and group 1 (MCA with plaque and without infarct) and between group 1 and group 2 (MCA with plaque and infarct). (A) Pairwise comparisons of C_{wk} between the MCA groups. (B) Pairwise comparisons of R between the MCA groups. (C) Pairwise comparisons of Q_{mean} between the MCA groups. (D) Pairwise comparisons of PI between the MCA groups. Adjusted for sex, hyperlipidemia, and diabetes in multivariate analysis. *, indicates a statistically significant difference, with P<0.05. AC and VR are represented as capacitance term C_{wk} and resistance term R, respectively. MCA, middle cerebral artery; AC, arterial compliance; VR, vascular resistance; Q_{mean}, mean blood flow; PI, pulsatility index.

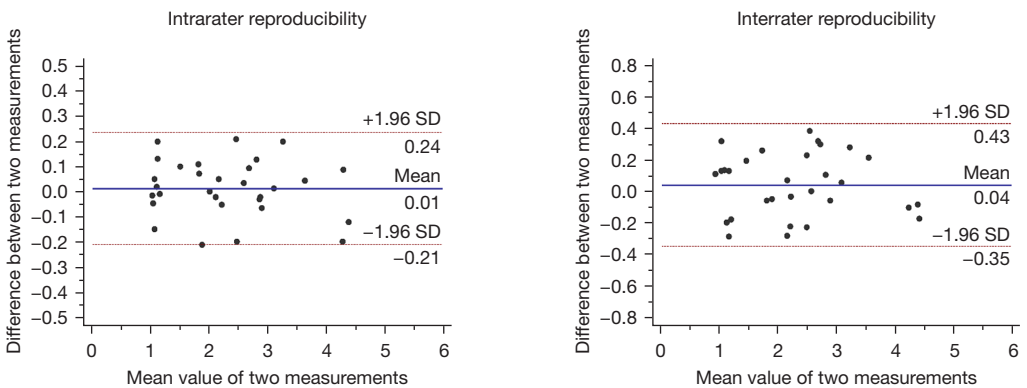

Figure 4 Bland-Altman plots showing intrarater and interrater reproducibility of flow measurements. In the analysis, Q_{mean} was used to validate the reproducibility of flow measurements. Q_{mean}, mean blood flow.

3 groups (8.86±2.42 *vs.* 15.29±4.26 *vs.* 22.47±8.82; P<0.001) as shown in *Table 1*. After adjustment for confounding factors, pairwise comparison of PWV_{AC} also showed significant differences between group 0 and group 1 (8.86±2.42 *vs.* 15.29±4.26; OR =1.726; P<0.001) and between group 1 and group 2 (15.29±4.26 *vs.* 22.47±8.82; OR =1.196; P=0.004).

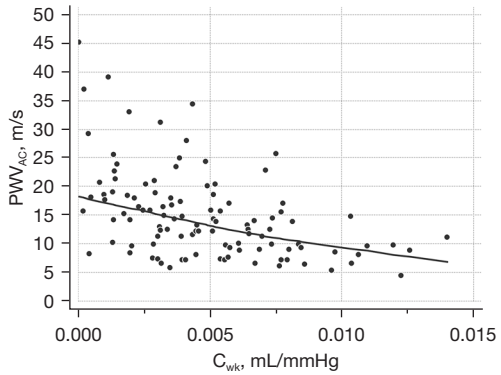

Figure 5 Correlation between 2 measures of arterial stiffness. Scatter plot of C_{wk} (mL/mmHg) and PWV_{AC} (m/s). AC and VR are represented as capacitance term C_{wk} and resistance term R, respectively. PWV_{AC}, pulse wave velocity; AC, arterial compliance; VR, vascular resistance.

Correlation between Cwk and PWVAC

The results showed that C_{wk} and PWV_{AC} were moderately correlated, with a correlation coefficient of −0.4736 ($P<0.001$). The scatter plot of the result is shown in *Figure 5*.

Discussion

In this study, we use a noninvasive method based on 4D flow MRI and the Windkessel model to evaluate the AC, VR, Q_{mean}, and PI of the MCA territory. Comparison of these features was conducted among 3 MCA groups according to plaque and infarct, and significant differences were found in all these features. From group 0 to group 2, AC and Q_{mean} decreased while VR increased. PI showed no unidirectional tendency, and the PI of group 1 (MCA with plaque but without infarct) was the highest among the 3 groups. The PI of group 0 was in line with previous studies (17). PI is age-related (4), and the PI in group 0 in this study was consistent with the age-matched control group reported in a previous study of MCA (mean age =56 years; PI =0.8±0.2).

Feature alterations due to plaque were investigated with a comparison between group 0 (MCA without plaque) and group 1 (MCA with plaque and without infarct). The results demonstrated that compared with group 0, group 1 had a lower AC, higher VR, significantly reduced Q_{mean}, and a higher PI. This can be attributed to the components and changes of the arterial walls. Arterial walls are mainly composed of 3 layers—the intima, media, and adventitia—of which the media contributes most to the AC. The media consists of elastic fibers, collagen fibers, and vascular smooth muscle cells. Due to aging or cardiovascular diseases, the media undergoes structural dysfunctions, such as elastin fragmentation, calcium deposition, and increased collagen: elastin ratios, which can result in reduced AC (3,6,27). The pathological changes of ICAD include intimal necrosis and thickening, neovascularization, and calcium deposition in the degenerated media (28). The presence of atherosclerotic plaques impairs the elastic properties of the arterial wall (10), resulting in a reduced AC. According to Poiseuille's law, VR, which reflects the impedance of the vascular system, is approximately inversely proportional to the fourth power of the vascular radius (7,29). VR increases when vasoconstriction and decreases due to vasodilation, which is regulated by both arterioles and large cerebral arteries (29,30). Based on this theory, VR is thought to increase with luminal stenosis or infarct due to atherosclerotic plaque, which is in accordance with our results. Q_{mean} was smaller in group 1 than in group 0. As mentioned above, the VR of group 1 increased, and this resulted in its reduced blood flow. The PI was higher in group 1 than in group 0, because group 1 had a reduced AC and higher VR that led to impaired regulation functions smoothing out pulsatility.

Feature alterations due to infarct were investigated in groups with MCA atherosclerotic plaque, via a comparison between group 1 (MCA with plaque and without infarct) and group 2 (MCA with plaque and infarct). Compared with group 1, group 2 had a significantly smaller AC, higher VR, decreased Q_{mean}, and a lower PI. The results indicated that atherosclerotic MCAs with infarct in the supplying territories tended to be stiffer than those without infarct. MCA atherosclerotic plaques with corresponding downstream infarct (or culprit plaques) are typically more unstable than are those without infarct (nonculprit lesion), and unstable plaques are associated with composition changes, such as intraplaque hemorrhage (31). Previous studies have indicated that some of these features are associated with reduced AC (9,10), and this likely explains why the AC of group 2 was smaller than that of group 1. As for VR, compared with group 1, group 2 had a higher R value. With the occurrence of infarct in the MCA territory, the impedance of the vascular system increases, with VR increasing in turn (7). With an increased R, blood flow decreased, so Q_{mean} of group 2 was smaller than that of group 1. The PI variation between group 1 and group 2 MCA was due to the combined action of AC and VR. Using Eq. [1] and Eq. [3] in Eq. [2], we can express PI as Eq. [6]:

$$PI = \frac{PP_{MCA}}{MAP_{MCA}} \sqrt{(\omega RC)^2 + 1} \quad [6]$$

Based on Eq. (6), PI is nonlinearly proportional to the product of R and C. In the comparison of the PI values between the MCA groups, the critical parameters were R and C because the pressure difference among the 3 groups was not significantly different (*Table 1*). In the comparison of group 2 (MCA with infarct) with group 1 (MCA without infarct), group 2 had a significantly increased R and a more significantly decreased C, resulting in a smaller product of R and C. This is likely why the PI in the MCA with infarct group (group 2) was smaller than that of the MCA without infarct group (group 1). Therefore, combined with above PI comparison between group 0 and 1, we determined that the PI of group 1 MCA was the highest among the 3 MCA groups.

Changes in hemodynamics and the vascular system functions also affect disease progression and patient prognosis, especially in atherosclerosis. The relationship between hemodynamics, vascular function, and disease progression could possibly be mutual. On the one hand, the occurrence of atherosclerosis may reduce the AC and raise blood flow pulsatility. On the other hand, higher blood flow pulsatility promotes vascular impairment, which is a precursor to atherosclerosis and results in reduced AC. Once the vicious cycle is initiated, these factors interact and disease progression ensues (32). Other evidence suggests that PI is correlated with future stroke risk and may play an important role in the development of stroke (33). One study also found arterial stiffness to be an important determinant of intraplaque hemorrhage (10), indicating the function of AC in atherosclerosis progression. In summary, hemodynamics and vascular function may also influence disease progression and clinical prognosis, especially in cases of atherosclerosis. Research into the bidirectional relation of factors including hemodynamics, vascular function, and atherosclerosis may thus be warranted.

There were significant differences in the occurrence of hyperlipidemia among the 3 groups. Hyperlipidemia, especially hypercholesterolemia (elevated LDL-C), is one of the most prevalent risk factors leading to the progression of atherosclerosis (34). As can be seen in *Table 1*, the percentage of hyperlipidemia of group 1 (MCA with plaque and without infarct) was higher than that in group 0 (MCA without plaque). The difference between group 0 and group 1 may point to a link between hyperlipidemia and atherosclerosis, which is consistent with a previous study (35). Due to the small sample size, group 2 (MCA with plaque and infarct) had a relatively smaller percentage of hyperlipidemia. Adjustments for hyperlipidemia were conducted in the comparison of AC, VR, Q_{mean}, and PI among the 3 groups.

This study had several limitations. First, each MCA group was represented by a small sample. Differences in AC, VR, and PI among MCA groups need to be investigated in a larger cohort with a more balanced dataset in terms of demographic and clinical information. In this study, the confounding factors including sex and hyperlipidemia were adjusted in pairwise comparisons of the MCA groups. Second, our model assumed that corresponding blood pressure into the MCA vascular system is 0.7 times the value of SBP and DBP, but this ratio may vary across individuals. Considering the ratio of 0.7 was based on values in previous studies, we can assume that the results can reliably reflect an average level. Third, the Windkessel model is one indirect lumped measurement of vessel properties, so it is limited in simulating pulse waves and calculating the local vessel properties. Fourth, lifestyle risk factors associated with ICAD, such as physical activity or obesity, were not examined in this study.

Conclusions

The presence of intracranial atherosclerotic plaque or infarct is associated with decreased AC and increased VR in ICAD. Moreover, from the conditions of no plaque, to plaque, and to plaque with infarct, AC and blood flow decreased while VR increased. As for PI, it increased in the presence of plaque but decreased in the presence of infarct, with the PI being highest in the condition with plaque and no infarct. Assessments of arterial function and hemodynamics in a single intracranial artery territory can clarify the overall CVS alterations due to plaque and infarct in ICAD. This work clarifies the relationships between MCA vessel properties, plaque, and infarct, which may potentially have implications for the prognosis and risk determination of stroke.

Acknowledgments

Funding: This work was supported by the Beijing Municipal Science & Technology Commission (No. Z171100001017019) and the Tsinghua University Initiative Scientific Research Program (No. 20219990033).

Footnote

Reporting Checklist: The authors have completed the STROBE reporting checklist. Available at https://qims.amegroups.com/article/view/10.21037/qims-23-222/rc

Conflicts of Interest: All authors have completed the ICMJE uniform disclosure form (available at https://qims.amegroups.com/article/view/10.21037/qims-23-222/coif). The authors have no conflicts of interest to declare.

Ethical Statement: The authors are accountable for all aspects of the work in ensuring that questions related to the accuracy or integrity of any part of the work are appropriately investigated and resolved. The Ethics Review Board of the Beijing Tsinghua Changgung Hospital approved the study, and it was performed in accordance with the guidelines of the Declaration of Helsinki (as revised in 2013). Written informed consent was obtained from each patient or their legal guardians.

References

1. van den Beukel TC, van der Toorn JE, Vernooij MW, Kavousi M, Akyildiz AC, de Jong PA, van der Lugt A, Ikram MK, Bos D. Morphological Subtypes of Intracranial Internal Carotid Artery Arteriosclerosis and the Risk of Stroke. Stroke 2022;53:1339-47.
2. Syeda B, Gottsauner-Wolf M, Denk S, Pichler P, Khorsand A, Glogar D. Arterial compliance: a diagnostic marker for atherosclerotic plaque burden? Am J Hypertens 2003;16:356-62.
3. Lyle AN, Raaz U. Killing Me Unsoftly: Causes and Mechanisms of Arterial Stiffness. Arterioscler Thromb Vasc Biol 2017;37:e1-e11.
4. Zarrinkoob L, Ambarki K, Wåhlin A, Birgander R, Carlberg B, Eklund A, Malm J. Aging alters the dampening of pulsatile blood flow in cerebral arteries. J Cereb Blood Flow Metab 2016;36:1519-27.
5. Malek AM, Alper SL, Izumo S. Hemodynamic shear stress and its role in atherosclerosis. JAMA 1999;282:2035-42.
6. Marchais SJ, Guerin AP, Pannier B, Delavaud G, London GM. Arterial compliance and blood pressure. Drugs 1993;46 Suppl 2:82-7.
7. Westerhof N, Lankhaar JW, Westerhof BE. The arterial Windkessel. Med Biol Eng Comput 2009;47:131-41.
8. Švec D, Javorka M. Noninvasive arterial compliance estimation. Physiol Res 2021;70:S483-94.
9. Coutinho T, Yam Y, Chow BJW, Dwivedi G, Inácio J. Sex Differences in Associations of Arterial Compliance With Coronary Artery Plaque and Calcification Burden. J Am Heart Assoc 2017;6:e006079.
10. Selwaness M, van den Bouwhuijsen Q, Mattace-Raso FU, Verwoert GC, Hofman A, Franco OH, Witteman JC, van der Lugt A, Vernooij MW, Wentzel JJ. Arterial stiffness is associated with carotid intraplaque hemorrhage in the general population: the Rotterdam study. Arterioscler Thromb Vasc Biol 2014;34:927-32.
11. Navarro-Orozco D, Sánchez-Manso JC. Neuroanatomy, Middle Cerebral Artery. StatPearls. Treasure Island (FL): StatPearls Publishing Copyright © 2022, StatPearls Publishing LLC.; 2022.
12. Nogles TE, Galuska MA. Middle Cerebral Artery Stroke. StatPearls. Treasure Island (FL): StatPearls Publishing Copyright © 2022, StatPearls Publishing LLC.; 2022.
13. Li ML, Xu WH, Song L, Feng F, You H, Ni J, Gao S, Cui LY, Jin ZY. Atherosclerosis of middle cerebral artery: evaluation with high-resolution MR imaging at 3T. Atherosclerosis 2009;204:447-52.
14. Bikia V, Rovas G, Pagoulatou S, Stergiopulos N. Determination of Aortic Characteristic Impedance and Total Arterial Compliance From Regional Pulse Wave Velocities Using Machine Learning: An in-silico Study. Front Bioeng Biotechnol 2021;9:649866.
15. Lilly SM, Jacobs D, Bluemke DA, Duprez D, Zamani P, Chirinos J. Resistive and pulsatile arterial hemodynamics and cardiovascular events: the Multiethnic Study of Atherosclerosis. J Am Heart Assoc 2014;3:e001223.
16. Holmgren M, Wåhlin A, Dunås T, Malm J, Eklund A. Assessment of Cerebral Blood Flow Pulsatility and Cerebral Arterial Compliance With 4D Flow MRI. J Magn Reson Imaging 2020;51:1516-25.
17. Rivera-Rivera LA, Turski P, Johnson KM, Hoffman C, Berman SE, Kilgas P, Rowley HA, Carlsson CM, Johnson SC, Wieben O. 4D flow MRI for intracranial hemodynamics assessment in Alzheimer's disease. J Cereb

Blood Flow Metab 2016;36:1718-30.
18. Markl M, Frydrychowicz A, Kozerke S, Hope M, Wieben O. 4D flow MRI. J Magn Reson Imaging 2012;36:1015-36.
19. National Cholesterol Education Program (NCEP) Expert Panel on Detection, Evaluation, and Treatment of High Blood Cholesterol in Adults (Adult Treatment Panel III). Third Report of the National Cholesterol Education Program (NCEP) Expert Panel on Detection, Evaluation, and Treatment of High Blood Cholesterol in Adults (Adult Treatment Panel III) final report. Circulation 2002;106:3143-421.
20. Expert Panel on Detection, Evaluation, and Treatment of High Blood Cholesterol in Adults. Executive Summary of The Third Report of The National Cholesterol Education Program (NCEP) Expert Panel on Detection, Evaluation, And Treatment of High Blood Cholesterol In Adults (Adult Treatment Panel III). JAMA 2001;285:2486-97.
21. Leng X, Scalzo F, Ip HL, Johnson M, Fong AK, Fan FS, Chen X, Soo YO, Miao Z, Liu L, Feldmann E, Leung TW, Liebeskind DS, Wong KS. Computational fluid dynamics modeling of symptomatic intracranial atherosclerosis may predict risk of stroke recurrence. PLoS One 2014;9:e97531.
22. Tatu L, Moulin T, Bogousslavsky J, Duvernoy H. Arterial territories of the human brain: cerebral hemispheres. Neurology 1998;50:1699-708.
23. Li Y, Chen H, He L, Cao X, Wang X, Chen S, Li R, Yuan C. Hemodynamic assessments of venous pulsatile tinnitus using 4D-flow MRI. Neurology 2018;91:e586-93.
24. Leng X, Wong KS, Liebeskind DS. Evaluating intracranial atherosclerosis rather than intracranial stenosis. Stroke 2014;45:645-51.
25. Leng X, Lan L, Ip HL, Abrigo J, Scalzo F, Liu H, et al. Hemodynamics and stroke risk in intracranial atherosclerotic disease. Ann Neurol 2019;85:752-64.
26. Alhalimi T, Lim J, Gourley D, Tanaka H. Converting and Standardizing Various Measures of Arterial Stiffness to Pulse Wave Velocity. Pulse (Basel) 2021;9:72-82.
27. Springo Z, Toth P, Tarantini S, Ashpole NM, Tucsek Z, Sonntag WE, Csiszar A, Koller A, Ungvari ZI. Aging impairs myogenic adaptation to pulsatile pressure in mouse cerebral arteries. J Cereb Blood Flow Metab 2015;35:527-30.
28. Qureshi AI, Caplan LR. Intracranial atherosclerosis. Lancet 2014;383:984-98.
29. Delong C, Sharma S. Physiology, Peripheral Vascular Resistance. StatPearls. Treasure Island (FL): StatPearls Publishing Copyright © 2022, StatPearls Publishing LLC.; 2022.
30. Faraci FM, Heistad DD. Regulation of large cerebral arteries and cerebral microvascular pressure. Circ Res 1990;66:8-17.
31. Wang Y, Liu X, Wu X, Degnan AJ, Malhotra A, Zhu C. Culprit intracranial plaque without substantial stenosis in acute ischemic stroke on vessel wall MRI: A systematic review. Atherosclerosis 2019;287:112-21.
32. Dart AM, Kingwell BA. Pulse pressure--a review of mechanisms and clinical relevance. J Am Coll Cardiol 2001;37:975-84.
33. Chuang SY, Cheng HM, Bai CH, Yeh WT, Chen JR, Pan WH. Blood Pressure, Carotid Flow Pulsatility, and the Risk of Stroke: A Community-Based Study. Stroke 2016;47:2262-8.
34. Hill MF, Bordoni B. Hyperlipidemia. StatPearls. Treasure Island (FL): StatPearls Publishing Copyright © 2023, StatPearls Publishing LLC.; 2023.
35. Miao J, Zang X, Cui X, Zhang J. Autophagy, Hyperlipidemia, and Atherosclerosis. Adv Exp Med Biol 2020;1207:237-64.

Cite this article as: Chen W, Song X, Wei H, Fu M, Chen S, Wei C, Zheng Z, Wu J, Li R. Variations of arterial compliance and vascular resistance due to plaque or infarct in a single vascular territory of the middle cerebral artery. Quant Imaging Med Surg 2023;13(12):7802-7813. doi: 10.21037/qims-23-222

